Lecture Notes in Mechanical Engineering

S. A. Sannasiraj
S. Murty Bhallamudi
Panneer Selvam Rajamanickam
Deepak Kumar *Editors*

# Riverine, Estuarine and Marine Hydraulics

## Proceedings of Congress of the International Association for Hydraulic Environmental Engineering and Research-Asia Pacific Division

Springer

# Numerical Simulation of Submerged Hydraulic Jump Using a Urans Model


**Seongwook Choi and Sung-Uk Choi**

**Abstract** This paper presents numerical simulations of the submerged jump of the flow passing under a sluice gate. The 2D unsteady Navier–Stokes equations are solved with the $k-\omega$ SST (Shear Stress Transport) turbulence model. The volume of fluid method is used to compute the free surface and the water–air multiphase flow. The numerical model is applied to an experimental case. The mean flow and turbulence structures of the submerged jump are obtained, and their longitudinal decays are estimated. The computed results agree well with the measured data. The peak streamwise mean velocity and the Reynolds stress decays in the longitudinal direction, mainly accelerated by the adverse pressure gradient. However, the presence of the vena contracta clearly affects the decays of the mean velocity and the peak Reynolds stress downstream of the sluice gate.

**Keywords** Submerged hydraulic jump · Numerical simulation · $k$–$\omega$ SST model · Sluice gate · Longitudinal decay

## 1 Introduction

The free jumps are very efficient in dissipating the kinetic energy. The free jump is called the optimum jump when the toe of the jump located at the sluice gate, showing the best efficiency. If the tailwater level is raised further, then the submerged hydraulic jump is created from the free jump. The submerged jump dissipates less kinetic energy compared with the free jump. Typically, the flow structure of the submerged hydraulic jump is complicated, an extended wall jet region below a recirculatory region.

The submerged hydraulic jump creates an extended roller length with strong recirculating flows under the relatively calm free surface. This makes extremely

S. Choi
Senior Researcher, Department of Hydro Science and Engineering Research, Korea Institute of Civil Engineering and Building Technology, Goyang, Korea

S. Choi · S.-U. Choi (✉)
Department of Civil and Environmental Engineering, Yonsei University, Seoul, Korea
e-mail: schoi@yonsei.ac.kr



S. A. Sannasiraj et al. (eds.), *Riverine, Estuarine and Marine Hydraulics*, Lecture Notes in Mechanical Engineering, https://doi.org/10.1007/978-981-97-6009-1_1

dangerous situations for the swimmers to be drowned by being captured by the fierce vortical flows. Air entrainment into the submerged jump is less than the free jump because the body of the submerged jump is not directly exposed to air. The submerged jump induces much less pressure fluctuations on the bed than the free jump does.

This study presents numerical simulations of the submerged jump of the flow passing under the sluice gate. For the numerical simulations, 2D Unsteady Reynolds-Averaged Navier–Stokes (URANS) equations are solved with the $k-\omega$ SST turbulence model. The volume of fluid (VOF) method is used to track the free surface and to compute the water–air multiphase flow. The numerical model is applied to an experimental case of [4]. The computed vertical structures of the mean flow and turbulence statistics and their decaying rates are presented and compared with measured data in the literature.

## 2 Governing Equations

The following URANS equation is solved for computing the flow passing under a sluice gate:

$$\frac{\partial \rho}{\partial t} + \frac{\partial \rho \tilde{u}_i}{\partial x_i} = 0 \tag{1}$$

$$\frac{\partial \rho \tilde{u}_i}{\partial t} + \frac{\partial \rho \tilde{u}_i \tilde{u}_j}{\partial x_j} = -\frac{\partial \tilde{p}}{\partial x_i} + \frac{1}{\partial x_j}\left\{(\mu + \mu_t)\frac{\partial \tilde{u}_i}{\partial x_j}\right\} + \rho g_i \tag{2}$$

where $\tilde{u}_i$ is ensemble averaged velocity of $x_i$-direction, $t$ is time, $\rho$ is density of mixture, $\tilde{p}$ is ensemble averaged pressure, $\mu$ is viscosity of water–air mixture, $\mu_t$ is turbulent viscosity, and $g$ is gravitational acceleration. The VOF method is used to predict the free surface [1]. The VOF method solves the transport equation of volume fraction ($\alpha$) such as

$$\frac{\partial \alpha}{\partial t} + \frac{\partial \alpha \tilde{u}_i}{\partial x_i} = 0 \tag{3}$$

The region where $\alpha$ is between 0 and 1, which represents states fully occupied by air and water, respectively.

## 3 Turbulence Model

Turbulent viscosity can be estimated by the $k$–$\omega$ SST turbulence model [5] such as

$$\mu_t = \frac{a_1 \rho k}{\max(a_1 \omega, \overline{S} F_2)} \tag{4}$$

where $k$ is turbulence kinetic energy, $\omega$ is specific dissipation rate of $k$, $\overline{S}$ is the strain rate of the flow, $F_2$ is blending function, and $a_1$ is model coefficient. From the $k$–$\omega$ SST model, $k$ and $\omega$ can be obtained by solving the following respective transport equations:

$$\frac{\partial k}{\partial t} + \tilde{u}_j \frac{\partial k}{\partial x_j} = \frac{1}{\partial x_j}\left\{(\nu + \sigma_k \nu_t)\frac{\partial k}{\partial x_j}\right\} + P_k - \beta^* k\omega \tag{5}$$

$$\frac{\partial \omega}{\partial t} + \tilde{u}_j \frac{\partial \omega}{\partial x_j} = \frac{1}{\partial x_j}\left\{(\nu + \sigma_\omega \nu_t)\frac{\partial \omega}{\partial x_j}\right\} + \alpha_1 \overline{S}^2 - \beta\omega^2 + 2(1 - F_1)\sigma_{\omega 2}\frac{1}{\omega}\frac{\partial k}{\partial x_i}\frac{\partial \omega}{\partial x_i} \tag{6}$$

where $\nu$ is the kinematic viscosity of the water–air mixture, $\nu_t$ is the turbulent kinematic viscosity, $P_k$ is the production term of $k$, $\sigma_k$, $\sigma_\omega$, $\alpha_1$, $\beta^*$, $\beta$, and $\sigma_{\omega 2}$ are model coefficients, and $F_1$ is a blending function. The model coefficients $\sigma_k$, $\sigma_\omega$, and $\beta$ are obtained through the blending function.

For calculating the velocity–pressure correlation, pisoFoam in OpenFOAM [2] based on the PISO algorithm is used. The time derivative terms are discretized by Euler scheme. The convection and the diffusion terms are discretized by the VanLeer scheme [6] and Gauss linear corrected scheme, respectively. All discretized terms are interpreted using the generalized geometric-algebraic multi-grid (GAMG) matrix solver.

## 4 Computational Condition

The flow condition comes from [4] experiments, where the inflow Froude number and the submergence factor are 8.19 and 0.24, respectively. As for the boundary conditions, the uniform bulk velocity is imposed at the inlet, and the no-slip boundary condition is used in the bed and the sluice gate. The free fall condition and Neumann boundary condition are used at the outlet and for the upper boundary, respectively. For the computational grid, uniform cells of 10 mm size are used except for the region close to the bed, where finer cells of 1 mm are used.

## 5 Vertical Structures

The computed results of mean flow and turbulence characteristics are presented and compared with measured data in [4]. Figure 1 shows the distributions of the streamwise mean velocity at some longitudinal distances in the developed zone for

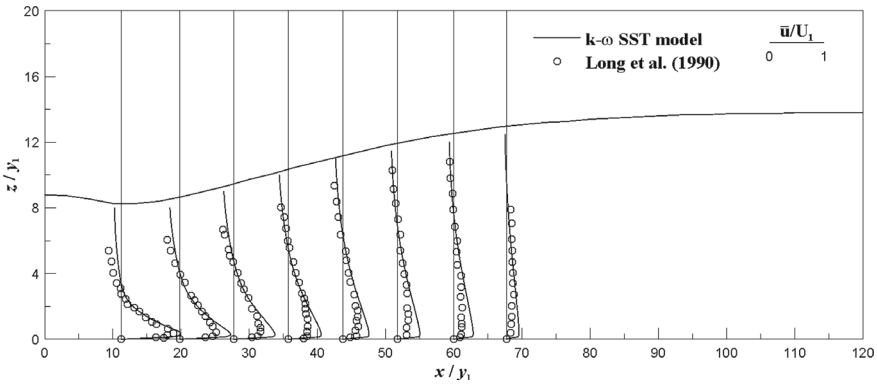


**Fig. 1** Distribution of streamwise mean velocity

the submerged jump. The streamwise mean velocity and distance in the axis are normalized by the bulk velocity and flow depth at the $x = 0$, respectively. In the figure, the computed results are given with the measured data. Basically, the velocity profiles show the re-circulating flows over the wall-jet-like flow in the developed zone. The maximum velocity of wall-jet-like flow and reverse flow velocity decay with the longitudinal distance because of the adverse pressure gradient. In general, the computed results agree well with the measured data; however, the numerical model over-predict the velocity in the vicinity of the bed. This is due to that the measurements were not made at the center of the channel but at the section close to the side wall.

Figure 2 shows the distributions of the Reynolds stress at some longitudinal distances in the developed zone for the submerged jump. The Reynolds stress is normalized by the bulk velocity squared. In general, the computed results agree well with the measured data. In particular, the Reynolds stress has a small positive value in the region very close to the bed, decreasing to a negative peak and increasing gradually thereafter. The heights of zero Reynolds stress near the bed and negative peak roughly correspond to the peak of the streamwise mean velocity and the inflection point of the mean velocity profile, respectively. The magnitude of the negative peak of the Reynolds stress is largest at the location where the jump starts and decreases in the longitudinal direction, resulting zero at the end of the developed zone.

## 6 Decay of Vertical Structures

Figure 3 shows the longitudinal decay of the peak streamwise mean velocity. The streamwise mean velocity and the longitudinal distance are normalized by the bulk velocity at the sluice gate and the distance where the peak streamwise mean velocity becomes the half of the bulk velocity, respectively. In the figure, the results from

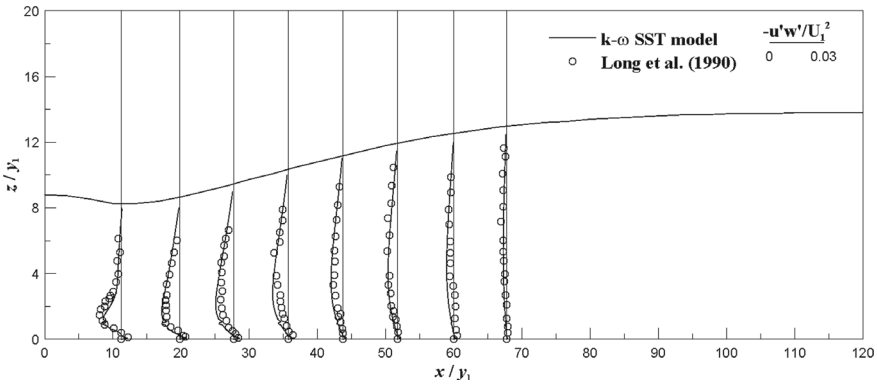


**Fig. 2** Distribution of Reynolds stress

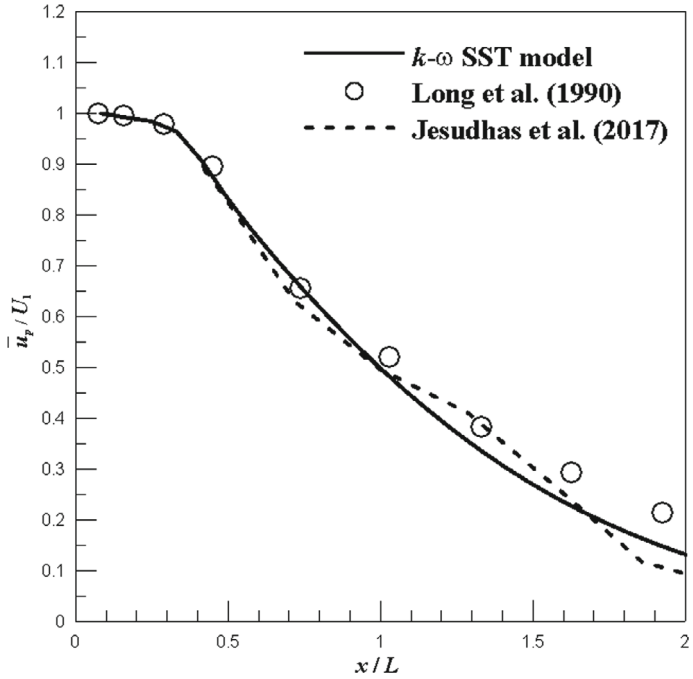


**Fig. 3** Longitudinal change of peak streamwise mean velocity

the numerical simulation by [3] are also given for comparisons. The figure reveals that the peak streamwise mean velocity decays rather non-linearly with time and the numerical model predicts well the longitudinal decay of the peak streamwise mean velocity. The decay of the peak streamwise mean velocity is very slowly for $x/L < 0.3$

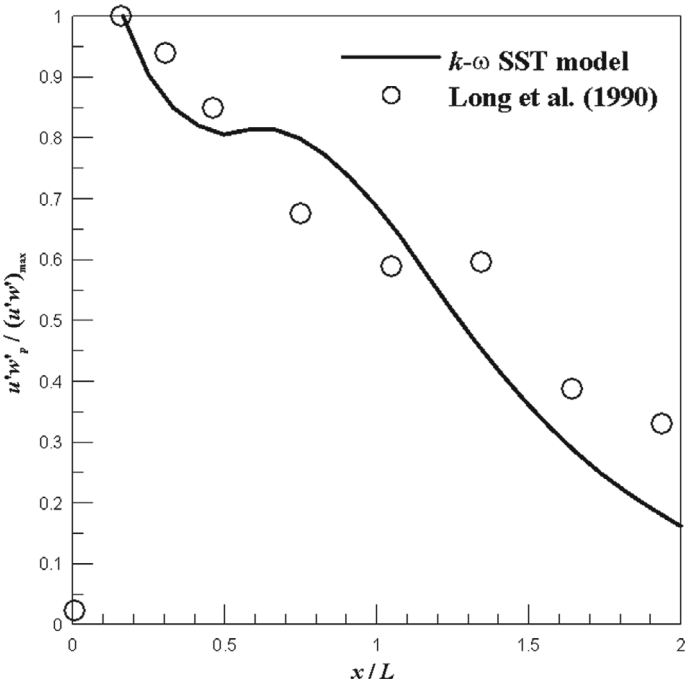


**Fig. 4** Longitudinal change of peak Reynolds stress

because of the vena contracta effect from the sluice gate. The decay of the streamwise mean velocity is fast and linear for $x/L < 1.2$, but is slowed down afterward.

Figure 4 shows the longitudinal decay of the peak Reynolds stress. The peak Reynolds stress is normalized by the maximum peak Reynolds stress. The computed result indicates that the peak Reynolds stress decays initially but does not decay in the range of $0.5 < x/L < 0.7$. Then the peak Reynolds stress decays continuously in the longitudinal direction. The suspension of the decay of the peak Reynolds stress is due to the presence of the vena contracta downstream of the sluice gate.

## 7 Conclusions

This study presented numerical simulations of the submerged hydraulic jump of the flow passing under the sluice gate. The URANS equations were solved with the $k$–$\omega$ SST turbulence model, and the VOF method was used to compute both the free surface and air–water mixture flow. The numerical model was applied to the experiments by [4], and the mean flow and turbulence statistics were presented.

The vertical structures of the streamwise mean velocity and Reynolds stress were provided and compared with measured data. It was found that the computed profiles agree well with measured data.

That is, the numerical model successfully reproduces the feature of the complicated flow structure, the wall jet flow below the recirculations. The longitudinal decays of the peak mean velocity and peak Reynolds stress were also given using the computed results. Moderate agreement was obtained by comparing the computed results and measured data. It was observed that both the mean velocity and Reynolds stress decay in the longitudinal direction, but their decay was clearly affected by the formation of the vena contracta downstream of the sluice gate.

**Acknowledgements** This work was supported by the National Research Foundation of Korea (NRF) grant funded by the Korea Government (NRF2020R1A2B5B01098937).

## References

1. Hirt CW, Nichols BD (1981) Volume of fluid (VOF) method for the dynamics of free boundaries. J Comput Phys 39(1):201–225
2. Jasak H (2009) OpenFOAM: open source CFD in research and industry. Int J Naval Archit Ocean Eng 1(2):88–94
3. Jesudhas V, Roussinova V, Balachandar R, Barron R (2017) Submerged hydraulic jump study using DES. J Hydraul Eng 143(3):04016091
4. Long D, Steffler PM, Rajaratnam N (1990) LDA study of flow structure in sub-merged hydraulic jump. J Hydraul Res 28(4):437–460
5. Menter FR (1992) Improved two-equation k-omega turbulence models for aerodynamic flows. NASA Ames Research Center, Moffett Field, CA
6. Van Leer B (1974) Towards the ultimate conservative difference scheme. II. Monotonicity and conservation combined in a second-order scheme. J Comput Phys 14(4):361–370